

Fermi National Accelerator Laboratory

FERMILAB-Pub-97/116-T

Finding Low-Scale Technicolor at Hadron Colliders

Estia Eichten and John Womersley

*Fermi National Accelerator Laboratory
P.O. Box 500, Batavia, Illinois 60510*

Kenneth Lane

*Department of Physics, Boston University
590 Commonwealth Avenue, Boston, MA 02215*

May 1997

Submitted to *Physics Letters*

Disclaimer

This report was prepared as an account of work sponsored by an agency of the United States Government. Neither the United States Government nor any agency thereof, nor any of their employees, makes any warranty, expressed or implied, or assumes any legal liability or responsibility for the accuracy, completeness, or usefulness of any information, apparatus, product, or process disclosed, or represents that its use would not infringe privately owned rights. Reference herein to any specific commercial product, process, or service by trade name, trademark, manufacturer, or otherwise, does not necessarily constitute or imply its endorsement, recommendation, or favoring by the United States Government or any agency thereof. The views and opinions of authors expressed herein do not necessarily state or reflect those of the United States Government or any agency thereof.

Distribution

Approved for public release; further dissemination unlimited.

FERMILAB-PUB-97/116-T
 BUHEP-97-13
 hep-ph/9704455

Finding Low-Scale Technicolor at Hadron Colliders

Estia Eichten^{1*}, Kenneth Lane^{2†} and John Womersley^{1‡}

¹Fermilab, P.O. Box 500, Batavia, IL 60510

²Dept.of Physics, Boston University, 590 Commonwealth Avenue, Boston, MA 02215

April 30, 1997

Abstract

In multiscale and topcolor-assisted models of walking technicolor, relatively light spin-one techni-hadrons ρ_T and ω_T exist and are expected to decay as $\rho_T \rightarrow W\pi_T, Z\pi_T$ and $\omega_T \rightarrow \gamma\pi_T$. For $M_{\rho_T} \simeq 200$ GeV and $M_{\pi_T} \simeq 100$ GeV, these processes have cross sections in the picobarn range in $\bar{p}p$ collisions at the Tevatron and about 10 times larger at the Large Hadron Collider. We demonstrate their detectability with simulations appropriate to Run II conditions at the Tevatron.

*eichten@fnal.gov

†lane@buphyc.bu.edu

‡womersley@fnal.gov

1 Introduction

Light, color-singlet technipions, π_T^\pm and π_T^0 , are expected to occur in models of multiscale technicolor [1] and topcolor-assisted technicolor [2, 3, 4, 5]. These technipions will be resonantly produced via technivector meson dominance at substantial rates at the Tevatron and the Large Hadron Collider [6, 7]. The technivector mesons in question are an isotriplet of color-singlet ρ_T and the isoscalar partner ω_T . Because techni-isospin is likely to be a good approximate symmetry, ρ_T and ω_T should have equal masses as do the various technipions. The enhancement of technipion masses due to walking technicolor [8] suggest that the channels $\rho_T \rightarrow \pi_T \pi_T$ and $\omega_T \rightarrow \pi_T \pi_T \pi_T$ are closed. Thus, the decay modes $\rho_T \rightarrow W_L \pi_T$ and $Z_L \pi_T$, where W_L , Z_L are longitudinal weak bosons, and $\omega_T \rightarrow \gamma \pi_T$ may dominate [1]. We assume in this paper that π_T^0 decays into $b\bar{b}$. These heavy flavors, plus an isolated lepton or photon, provide the main signatures for these processes.

We present simulations of $\bar{p}p \rightarrow \rho_T^\pm \rightarrow W_L^\pm \pi_T^0$ and $\omega_T \rightarrow \gamma \pi_T^0$ for the Tevatron collider with $\sqrt{s} = 2 \text{ TeV}$ and an integrated luminosity of 1 fb^{-1} . For $M_{\rho_T} \simeq 200 \text{ GeV}$ and $M_{\pi_T} \simeq 100 \text{ GeV}$, cross sections at the Tevatron are expected to be several picobarns. The narrowness of the ρ_T and ω_T resonances suggests topological cuts that enhance the signal-to-background ratio. For the cross sections we assume in this paper, the signals stand out well above the background once a single b -tag is also required. Although we do not simulate these processes for the LHC, cross sections there are an order of magnitude larger than at the Tevatron, so detection of the light technihadrons should be easy. We focus first on ρ_T production and decay and take up the ω_T later.

2 $\rho_T^\pm \rightarrow W^\pm \pi_T^0$

In Ref. [6], we assumed that there is just one light isotriplet and isoscalar of color-singlet technihadrons and used a simple model of technirho production and decay to determine the rates of the processes

$$\begin{aligned} q\bar{q}' &\rightarrow W^\pm \rightarrow \rho_T^\pm \rightarrow W_L^\pm Z_L^0; \quad W_L^\pm \pi_T^0, \quad \pi_T^\pm Z_L^0; \quad \pi_T^\pm \pi_T^0 \\ q\bar{q} &\rightarrow \gamma, Z^0 \rightarrow \rho_T^0 \rightarrow W_L^+ W_L^-; \quad W_L^\pm \pi_T^\mp; \quad \pi_T^\pm \pi_T^\mp \end{aligned} \tag{1}$$

and their dependence on M_{ρ_T} . We found that the most important processes were those with positive $Q = M_{\rho_T} -$ (sum of final-state masses) and the fewest number of longitudinal weak bosons. For $M_{\rho_T} \lesssim 250$ GeV and $M_{\pi_T} \simeq 100$ GeV, the dominant processes have cross sections of 1–10 pb at the Tevatron and 10–100 pb at the LHC. The Q -values of the processes that dominate production typically are less than 30–40 GeV.

Technipion production at hadron colliders is based on a vector-meson-dominance model. The subprocess cross sections for a pair of technipions $\pi_A \pi_B$, including longitudinal weak bosons, are

$$\frac{d\hat{\sigma}(q_i \bar{q}_j \rightarrow \rho_T^{\pm,0} \rightarrow \pi_A \pi_B)}{d(\cos \theta)} = \frac{\pi \alpha^2 p_{AB}^3}{3 \hat{s}^{\frac{5}{2}}} \frac{M_{\rho_T}^4 \sin^2 \theta}{(\hat{s} - M_{\rho_T}^2)^2 + \hat{s} \Gamma_{\rho_T}^2(\hat{s})} A_{ij}^{\pm,0}(\hat{s}) \mathcal{C}_{AB}^2, \quad (2)$$

where α is the fine-structure constant, \hat{s} is the subprocess center-of-mass energy, p_{AB} is the technipion momentum, and θ is the π_A production angle in the subprocess c.m. frame. Ignoring Kobayashi-Maskawa mixing angles, the factors $A_{ij}^{\pm,0} = \delta_{ij} A_i^{\pm,0}$ are (for $\hat{s} \gg M_W^2, M_Z^2$)

$$\begin{aligned} A_i^{\pm}(\hat{s}) &= \frac{1}{4 \sin^4 \theta_W} \left(\frac{\hat{s}}{\hat{s} - M_W^2} \right)^2, \\ A_i^0(\hat{s}) &= |\mathcal{A}_{iL}(\hat{s})|^2 + |\mathcal{A}_{iR}(\hat{s})|^2; \\ \mathcal{A}_{iL}(\hat{s}) &= Q_i + \frac{2 \cos 2\theta_W}{\sin^2 2\theta_W} (T_{3i} - Q_i \sin^2 \theta_W) \left(\frac{\hat{s}}{\hat{s} - M_Z^2} \right), \\ \mathcal{A}_{iR}(\hat{s}) &= Q_i - \frac{2 Q_i \cos 2\theta_W \sin^2 \theta_W}{\sin^2 2\theta_W} \left(\frac{\hat{s}}{\hat{s} - M_Z^2} \right). \end{aligned} \quad (3)$$

Here, $Q_i = \frac{2}{3}, -\frac{1}{3}$ and $T_{3i} = \frac{1}{2}, -\frac{1}{2}$ are the electric charge and third component of weak isospin for (left-handed) quarks u_i and d_i , respectively.

The energy-dependent width $\Gamma_{\rho_T}(\hat{s})$ in Eq. (2) is given by the sum of the ρ_T partial widths to technipions $\pi_A \pi_B$ and to fermion pairs $\bar{f}_i f_j$. The former is

$$\Gamma(\rho_T \rightarrow \pi_A \pi_B) = \frac{2 \alpha_{\rho_T} \mathcal{C}_{AB}^2}{3} \frac{p_{AB}^3}{\hat{s}}, \quad (4)$$

where the coupling $\alpha_{\rho_T} = 2.91(3/N_{TC})$ is naively scaled from QCD. In calculations, we take the number of technicolors to be $N_{TC} = 4$. The parameter

\mathcal{C}_{AB}^2 depends on a mixing angle χ and is given by [6, 1]

$$\mathcal{C}_{AB}^2 = \begin{cases} \sin^4 \chi & \text{for } W_L^+ W_L^- \text{ or } W_L^\pm Z_L^0 \\ \sin^2 \chi \cos^2 \chi & \text{for } W_L^\pm \pi_T^\mp, W_L^\mp \pi_T^\pm \text{ or } W_L^\pm \pi_T^0, Z_L^0 \pi_T^\pm \\ \cos^4 \chi & \text{for } \pi_T^+ \pi_T^- \text{ or } \pi_T^\pm \pi_T^0 \end{cases} \quad (5)$$

Note that, for a given technirho, $\sum_{AB} \mathcal{C}_{AB}^2 = 1$. We take $\sin \chi = \frac{1}{3}$ in our calculations. The ρ_T are *very* narrow, $\Gamma(\rho_T \rightarrow \pi_A \pi_B) \lesssim 1 \text{ GeV}$ for $\sqrt{\hat{s}} = M_{\rho_T} \simeq 210 \text{ GeV}$. The decay rates of the ρ_T to fermion-antifermion states are even smaller and are given by

$$\Gamma(\rho_T^{\pm,0} \rightarrow \bar{f}_i f_j) = \frac{C_f \alpha^2 M_{\rho_T}^4}{3\alpha_{\rho_T} \hat{s}^2} \frac{p_i (2\hat{s}^2 - \hat{s}(m_i^2 + m_j^2) - (m_i^2 - m_j^2)^2)}{2\hat{s}^2} A_{ij}^{\pm,0}(\hat{s}), \quad (6)$$

where $C_f = 3$ (1) for color-triplet (singlet) final-state fermions; p_i is the momentum and m_i the mass of fermion f_i .

We focus on technirho decay modes with the best signal-to-background ratios, namely, $\rho_T \rightarrow W_L \pi_T$ or $Z_L \pi_T$. For definiteness, we assume $M_{\rho_T} = 210 \text{ GeV}$ and $M_{\pi_T} = 110 \text{ GeV}$. Technipion couplings to fermions are expected to be proportional to mass. We adhere to that expectation in this paper and assume that technipions decay as

$$\begin{aligned} \pi_T^0 &\rightarrow b\bar{b} \\ \pi_T^\pm &\rightarrow c\bar{b} \text{ or } c\bar{s}, \tau^\pm \nu_\tau. \end{aligned} \quad (7)$$

Thus, heavy-quark jet tagging is an important aid to technipion searches.¹

We have used PYTHIA 6.1 [9] to generate $\bar{p}p \rightarrow W^\pm \rightarrow \rho_T^\pm \rightarrow W^\pm \pi_T^0$ with $\pi_T^0 \rightarrow \bar{b}b$ at the Tevatron Collider with $\sqrt{s} = 2 \text{ TeV}$. The cross section for this process is 5.3 pb. We also used PYTHIA to generate the $W^\pm \text{jet jet}$ background. Jets were found using the clustering code provided in PYTHIA with a cell size of $\Delta\eta \times \Delta\phi = 0.1 \times 0.1$, a cone radius $R = 0.7$ and a minimum jet E_T of 5 GeV. Cell energies were smeared using a calorimeter resolution of $0.5\sqrt{E(\text{GeV})}$. Missing transverse energy \cancel{E}_T was then calculated as:

$$\cancel{E}_T = - \left| \sum_{\text{jets}, \ell^\pm} \mathbf{E}_T \right| \quad (8)$$

¹We note that some topcolor-assisted technicolor models [5] have the feature that certain technifermions, and their bound-state technipions, couple mainly to the lighter fermions of the first two generations. The flavor-blind kinematical cuts we discuss below will be essential for this possibility.

Selected events were required to have an isolated electron or muon, large missing energy, and two or more jets. The selection criteria were:

- Lepton: $E_T(\ell) > 25 \text{ GeV}$; pseudorapidity $|\eta| < 1.1$.
- Missing energy: $\cancel{E}_T > 25 \text{ GeV}$.
- Transverse mass: $50 \text{ GeV} < \mathcal{M}_T(\ell \cancel{E}_T) < 100 \text{ GeV}$.
- Two or more jets with $E_T > 20 \text{ GeV}$ and $|\eta| < 2.0$, separated from the lepton by at least $\Delta R = 0.7$.

Requiring that the lepton and jets be central in pseudorapidity exploits the fact that the signal events will tend to be produced with larger center-of-mass scattering angles than the background. Figure 1(a) shows the invariant mass distribution of the two highest- E_T jets for the signal (black) and background (grey) events passing these criteria for a luminosity of 1 fb^{-1} , half that expected in Tevatron Run II.

The peculiar kinematics of $\rho_T \rightarrow W_L \pi_T$ and $Z_L \pi_T$ suggest other cuts that can discriminate signals from the $W/Z + \text{jets}$ backgrounds.² The small Q -values for ρ_T decays causes the π_T and W_L (or Z_L) to have low transverse momenta, $p_T < p_T^{\text{max}} = \sqrt{M_{\rho_T}^4 - 2M_{\rho_T}^2(M_{\pi_T}^2 + M_W^2) + (M_{\pi_T}^2 - M_W^2)^2} \simeq 45 \text{ GeV}$ for our reference masses. Not only is the p_T of the dijet system limited, but the jets are emitted with an opening azimuthal angle $\Delta\phi(jj) \gtrsim 140^\circ$. These expectations were borne out by simulated distributions in these variables. Cutting on the maximum and minimum $p_T(jj)$ and the minimum $\Delta\phi(jj)$ help suppress the Wjj background to $\rho_T \rightarrow W_L \pi_T$.

Consequently, we have taken the selected events in Fig. 1(a) and applied the additional topological cuts $\Delta\phi(jj) > 125^\circ$ and $20 < p_T(jj) < 50 \text{ GeV}$. These cuts reject 78% of the Wjj background while retaining 64% of the signal. The results are shown in Fig. 1(b). For the signal cross section of 5.3 pb , the signal-to-background at 100 GeV is improved from 0.04 to 0.11 by these cuts. A signal rate in excess of 15 pb would produce a visible excess at this level.

²The following discussion applies to both the Tevatron and the LHC but, because of the smaller boost rapidities of the ρ_T at the Tevatron, signal events will be more central there. Cutting harder on rapidity for LHC events will improve signal-to-background; the higher cross section and luminosity at the LHC leave plenty of events.

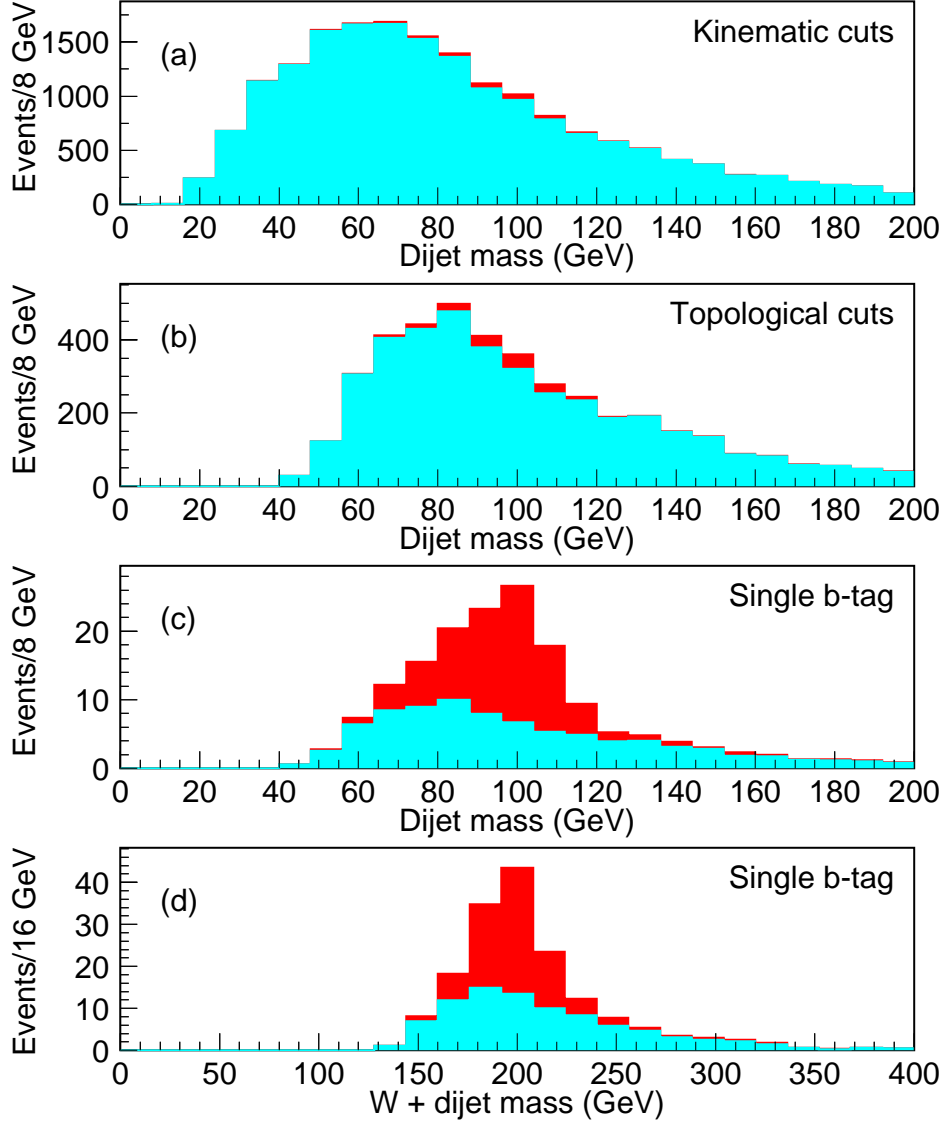


Figure 1: Invariant mass distributions for ρ_T signal (black) and Wjj background (grey); vertical scale is events per bin in 1 fb^{-1} of integrated luminosity. Dijet mass distributions (a) with kinematic selections only, (b) with the addition of topological selections, and (c) with the addition of single b -tagging; (d) W +dijet invariant mass distribution for the same sample as (c).

The additional effect of tagging one b -jet per event is shown in Fig. 1(c). We have assumed a 50% efficiency for tagging b 's, a 1% probability to mistag light quarks and gluons, and a 17% probability to mistag charm as a b . This final selection leaves a clear dijet resonance signal above the background at just below the mass of the π_T . For $80 < m_{jj} < 120$ GeV, there are 65 signal events over a background of 35. The mass distribution for the signal is almost gaussian, with a peak at 97 GeV and $\sigma \simeq 12.7$ GeV. This width and a tail on the low side are due mainly to the effects of final-state gluon radiation, fragmentation, calorimeter resolution and neutrinos from b -decay.

Figure 1(d) shows the invariant mass distributions for the Wjj system after topological cuts and b -tagging have been imposed. Here the W four-momentum was reconstructed from the lepton and \cancel{E}_T , taking the lower-rapidity solution in each case. Again, a clear peak is visible at just below the mass of the ρ_T . We point out that, especially after making the topological cuts, the dijet mass and the Wjj mass are highly correlated; a peak in one distribution is almost bound to correspond to a peak in the other. Thus, the existence of structure in both distributions does not add to the statistical significance of any observation.

We conclude that if ρ_T and π_T exist in the mass range we consider, they can be found without difficulty in Run II of the Tevatron. In fact, since there are ~ 65 signal events in Fig. 1(c) for $\sigma(\rho_T^\pm \rightarrow W^\pm \pi_T^0) \simeq 5$ pb, one might see hints of a signal with one tenth the luminosity. It is certainly worth looking in the presently accumulated samples of ~ 100 pb $^{-1}$ per experiment. The production cross section at 1.8 TeV is about 15% lower than at 2.0 TeV. Other channels may also add to the cross section: for our reference masses, $\rho_T^0 \rightarrow W^\pm \pi_T^\mp$ contributes an additional 2.3 pb, though only one b -jet is present in the π_T^\pm decay.

3 $\omega_T \rightarrow \gamma \pi_T^0$

We turn now to the signatures for ω_T production. The ω_T is produced in hadron collisions just as the ρ_T^0 , via its vector-meson-dominance coupling to γ and Z^0 . Its cross section is proportional to $|Q_U + Q_D|^2$, where $Q_{U,D}$ are the electric charges of the ω_T 's constituent technifermions. For $M_{\omega_T} \simeq M_{\rho_T}$, then, the ω_T and ρ_T^0 should be produced at comparable rates, barring accidental cancellations. If the $\rho_T \rightarrow \pi_T \pi_T$ channels are nearly or fully

closed, then $\omega_T \rightarrow \pi_T \pi_T \pi_T$ certainly is forbidden. If we can use decays of the ordinary ω as a guide, $\omega_T \rightarrow \gamma \pi_T^0$, $Z^0 \pi_T^0$ will be much more important than $\omega_T \rightarrow \pi_T \pi_T$ [6]. It is not possible to estimate the relative importance of these two modes without an explicit model, but it seems plausible that $\gamma \pi_T^0$ will dominate the phase-space-limited $Z^0 \pi_T^0$ channel. Therefore, we concentrate on the $\omega_T \rightarrow \gamma \pi_T^0 \rightarrow \gamma b \bar{b}$ mode in this paper. We shall find, surprisingly enough, that the decay modes $\omega_T \rightarrow \bar{q} q$ and $\ell^+ \ell^-$ decay modes are comparable to $\gamma \pi_T^0$.³

As for the technirho, the subprocess cross section for $\omega_T \rightarrow \gamma \pi_T^0$ production is obtained from a simple vector-meson-dominance model:

$$\frac{d\hat{\sigma}(q_i \bar{q}_i \rightarrow \omega_T \rightarrow \gamma \pi_T^0)}{d(\cos \theta)} = \frac{\pi \alpha^3 p^3}{12 \alpha_{\rho_T} M_T^2 \hat{s}^{\frac{3}{2}}} \frac{M_{\omega_T}^4 (1 + \cos^2 \theta)}{(\hat{s} - M_{\omega_T}^2)^2 + \hat{s} \Gamma_{\omega_T}^2(\hat{s})} B_i^0(\hat{s}), \quad (9)$$

where p is the photon momentum. The factor B_i is given by

$$\begin{aligned} B_i^0(\hat{s}) &= |\mathcal{B}_{iL}(\hat{s})|^2 + |\mathcal{B}_{iR}(\hat{s})|^2; \\ \mathcal{B}_{iL}(\hat{s}) &= \left[Q_i - \frac{4 \sin^2 \theta_W}{\sin^2 2\theta_W} (T_{3i} - Q_i \sin^2 \theta_W) \left(\frac{\hat{s}}{\hat{s} - M_Z^2} \right) \right] (Q_U + Q_D), \\ \mathcal{B}_{iR}(\hat{s}) &= \left[Q_i + \frac{4 Q_i \sin^4 \theta_W}{\sin^2 2\theta_W} \left(\frac{\hat{s}}{\hat{s} - M_Z^2} \right) \right] (Q_U + Q_D). \end{aligned} \quad (10)$$

Neglecting $\omega_T \rightarrow Z^0 \pi_T^0$, the energy-dependent width $\Gamma_{\omega_T}(\hat{s})$ in Eq. (9) is given by the sum of the partial widths

$$\begin{aligned} \Gamma(\omega_T \rightarrow \gamma \pi_T^0) &= \frac{\alpha p^3}{3 M_T^2}, \\ \Gamma(\omega_T \rightarrow \bar{f}_i f_i) &= \frac{C_f \alpha^2 M_{\omega_T}^4}{3 \alpha_{\rho_T} \hat{s}^2} \frac{p_i (\hat{s} - m_i^2)}{\hat{s}} B_i^0(\hat{s}). \end{aligned} \quad (11)$$

The mass parameter M_T in the $\omega_T \rightarrow \gamma \pi_T^0$ rate is unknown *a priori*; we take it to be $M_T = 100$ GeV in our calculations. We also took the technifermion charges to be $Q_U = \frac{4}{3}$ and $Q_D = Q_U - 1 = \frac{1}{3}$, and we used $M_{\omega_T} = M_{\rho_T} = 210$ GeV and $M_{\pi_T} = 110$ GeV.

³We thank Torbjorn Sjostrand for emphasizing to us the importance of the $\omega_T \rightarrow \ell^+ \ell^-$ channel.

Note that the decay rate for the $\gamma\pi_T^0$ mode is $\mathcal{O}(\alpha)$ and the differential subprocess cross section is nominally of $\mathcal{O}(\alpha^3)$. Nevertheless, the integrated $p^\pm p \rightarrow \omega_T \rightarrow \gamma\pi_T^0$ rate will be comparable to the rate for $p^\pm p \rightarrow \rho_T \rightarrow W_L\pi_T$ and $Z_L\pi_T$ if the $\gamma\pi_T^0$ mode dominates the ω_T width. Note also that the two rates in Eq. (11) are numerically comparable when summed over fermion flavors.

PYTHIA 6.1 [9] was used to generate $\bar{p}p \rightarrow \gamma, Z^0 \rightarrow \omega_T \rightarrow \gamma\pi_T^0$ with $\pi_T^0 \rightarrow \bar{b}b$ at $\sqrt{s} = 2\text{ TeV}$. The cross section for this process is 2.6 pb. The background considered is γjetjet . Selected events were required to have an isolated photon and two or more jets. The selection criteria were:

- Photon: $E_T(\gamma) > 50\text{ GeV}$; pseudorapidity $|\eta| < 1.1$.
- Two or more jets with $E_T > 20\text{ GeV}$ and $|\eta| < 2.0$, separated from the photon by at least $\Delta R = 0.7$.

Figure 2(a) shows the invariant mass distribution of the two highest- E_T jets for the signal (black) and background (grey) events passing these criteria for an integrated luminosity of 1 fb^{-1} . As for the ρ_T , backgrounds swamp the signal. Therefore, we have again investigated topological selections which might enhance the signal over the backgrounds. For $M_{\omega_T} \simeq 200\text{ GeV}$ and $M_{\pi_T} \simeq 100\text{ GeV}$, signal events have $p_T \lesssim 75\text{ GeV}$ and dijet azimuthal angle $\Delta\phi(jj) \gtrsim 105^\circ$. We apply the additional cut $\Delta\phi(jj) > 90^\circ$ to the untagged events of Fig. 2(a). However, no useful cut can be made on $p_T(jj)$ since the signal and background have very similar shapes.

The effect of these cuts is seen in Fig. 2(b). The γjj background is reduced by 61% while 75% of the signal is retained. Tagging one b -jet further improves the signal/background as shown in Fig. 2(c), and a clear peak just below the π_T mass can be seen. Figure 2(d) shows the photon+dijet invariant mass after the topological cuts and b -tagging are employed. Again, we found that this total invariant mass was not a useful variable to cut on.

In conclusion, we have shown that the low-scale technicolor signatures $\rho_T \rightarrow W\pi_T$ and $\omega_T \rightarrow \gamma\pi_T$ can be discovered easily in Run II of the Tevatron for production rates as low as a few picobarns. Low rates require b -tagging of the π_T . Topological cuts alone—which may be the only handle for technipions decaying to charmed or lighter quark jets—will be sufficient if cross sections exceed 10–15 pb. Signals with rates this large should be apparent in the

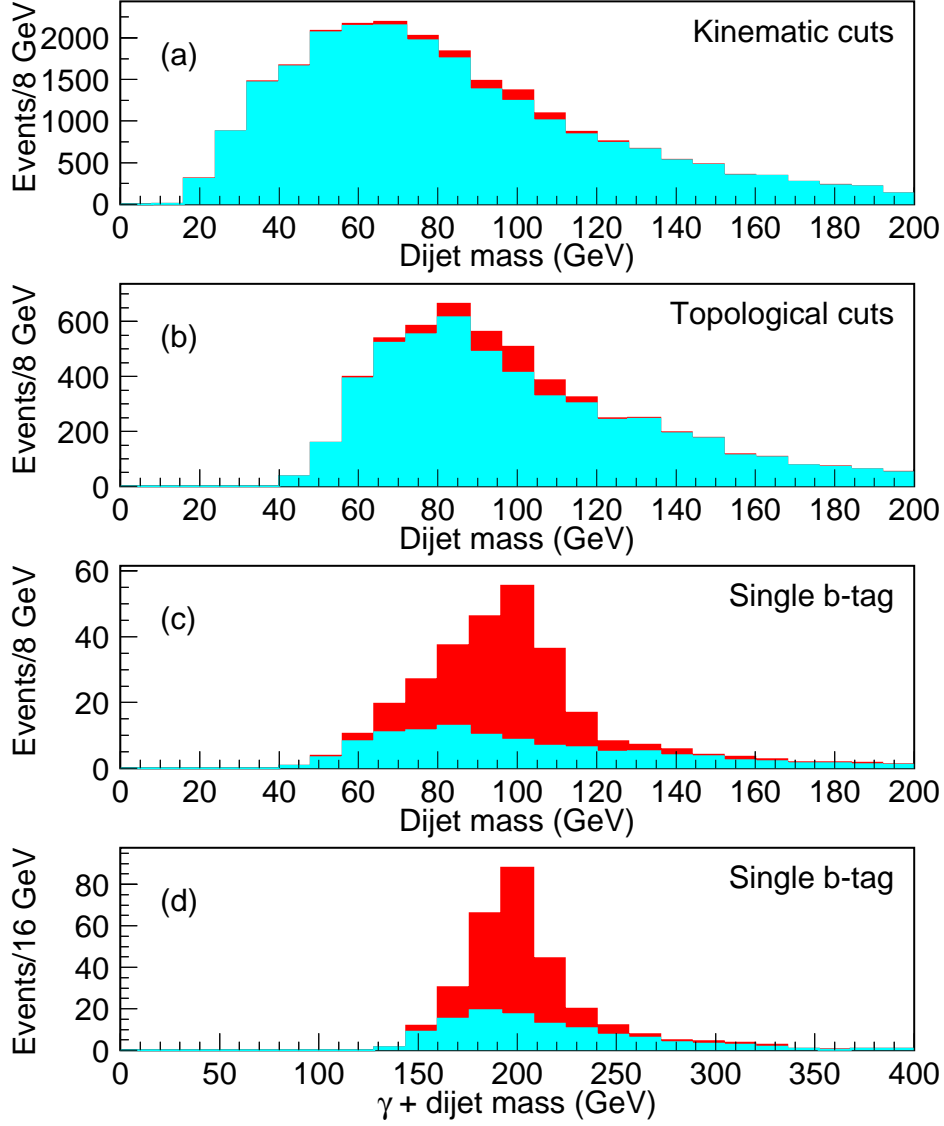


Figure 2: Invariant mass distributions for ω_T signal (black) and γjj background (grey); vertical scale is events per bin in 1 fb^{-1} of integrated luminosity. Dijet mass distributions (a) with kinematic selections only, (b) with the addition of topological selections, and (c) with the addition of single b -tagging; (d) $\gamma + \text{di jet}$ invariant mass distribution for the same sample as (c).

existing data. We urge that they be looked for. Production rates are an order of magnitude higher at the LHC than at the Tevatron. Thus, the LHC will be decisive in excluding low-scale technicolor signatures of the type considered here.

We are greatly indebted to Torbjorn Sjostrand for including the ρ_T and ω_T processes in PYTHIA and for many helpful and stimulating comments. The research of EE and JW is supported by the Fermi National Accelerator Laboratory, which is operated by Universities Research Association, Inc., under Contract No. DE-AC02-76CHO3000. KL's research is supported in part by the Department of Energy under Grant No. DE-FG02-91ER40676. KL thanks Fermilab for its hospitality during various stages of this work.

References

- [1] K. Lane and E. Eichten, Phys. Lett. **B222**, 274 (1989).
- [2] Y. Nambu, in *New Theories in Physics*, Proceedings of the XI International Symposium on Elementary Particle Physics, Kazimierz, Poland, 1988, edited by Z. Adjuk, S. Pokorski and A. Trautmann (World Scientific, Singapore, 1989); Enrico Fermi Institute Report EFI 89-08 (unpublished); V. A. Miransky, M. Tanabashi and K. Yamawaki, Phys. Lett. **221B**, 177 (1989); Mod. Phys. Lett. **A4**, 1043 (1989); W. A. Bardeen, C. T. Hill and M. Lindner, Phys. Rev. **D41**, 1647 (1990).
- [3] C. T. Hill, Phys. Lett. **266B**, 419 (1991) ; S. P. Martin, Phys. Rev. **D45**, 4283 (1992); *ibid* **D46**, 2197 (1992); Nucl. Phys. **B398**, 359 (1993); M. Lindner and D. Ross, Nucl. Phys. **B370**, 30 (1992); R. Bönisch, Phys. Lett. **268B**, 394 (1991); C. T. Hill, D. Kennedy, T. Onogi, H. L. Yu, Phys. Rev. **D47**, 2940 (1993).
- [4] C. T. Hill, Phys. Lett. **345B**, 483 (1995).
- [5] K. Lane and E. Eichten, Phys. Lett. **B352**, 382 (1995) ; K. Lane, Phys. Rev. **D54**, 2204 (1996).
- [6] E. Eichten and K. Lane, Phys. Lett. **B388**, 803 (1996).

- [7] E. Eichten and K. Lane, “Electroweak and Flavor Dynamics at Hadron Colliders–I”, FERMILAB-PUB-96/297-T, BUHEP-96-33, hep-ph/9609297; to appear in the proceedings of the 1996 DPF/DPB Summer Study on New Directions for High Energy Physics (Snowmass 96).
- [8] B. Holdom, Phys. Rev. **D24**, 1441 (1981); Phys. Lett. **150B**, 301 (1985); T. Appelquist, D. Karabali and L. C. R. Wijewardhana, Phys. Rev. Lett. **57**, 957 (1986); T. Appelquist and L. C. R. Wijewardhana, Phys. Rev. **D36**, 568 (1987); K. Yamawaki, M. Bando and K. Matumoto, Phys. Rev. Lett. **56**, 1335 (1986); T. Akiba and T. Yanagida, Phys. Lett. **169B**, 432 (1986).
- [9] T. Sjostrand, Comput. Phys. Commun. **82**, 74 (1994).